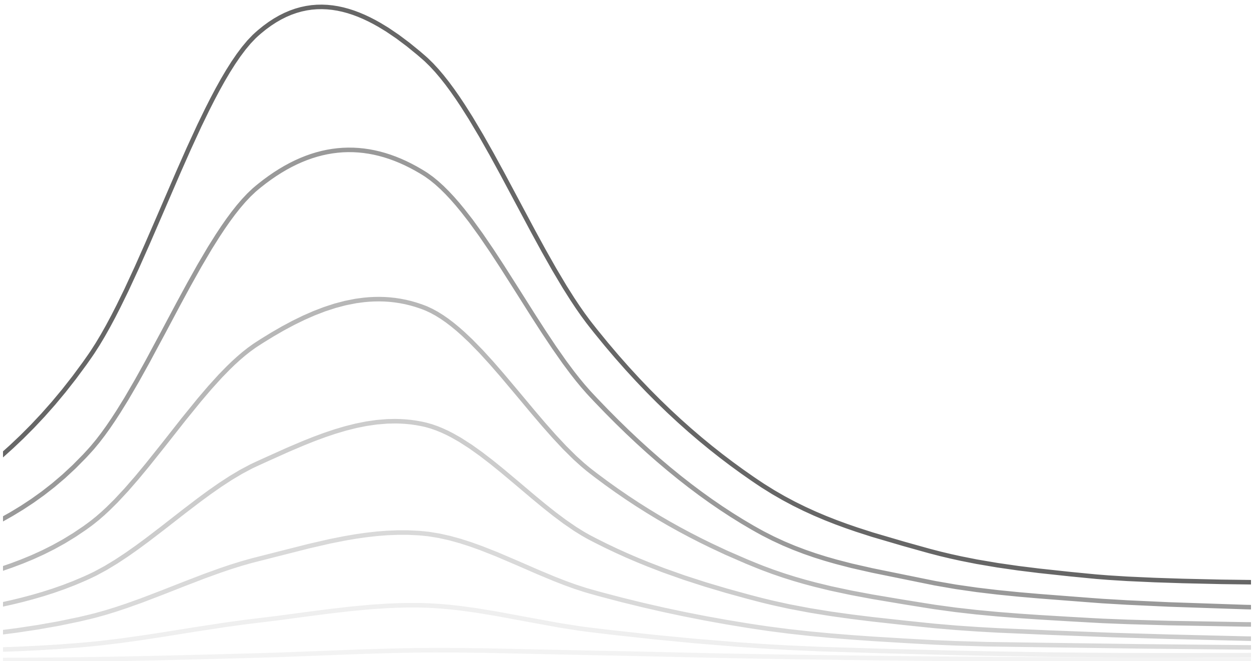

A Vibration-Powered Wireless Sensor Device for Machine Conditioning

Master's Thesis in Embedded Electronic System Design

ERIK ALMBRATT

RAKSHITHA BYADARAHALLI MADHUSUDHAN

Department of Computer Science and Engineering
CHALMERS UNIVERSITY OF TECHNOLOGY
UNIVERSITY OF GOTHENBURG
Gothenburg, Sweden 2022

Master's thesis 2022

A Vibration-Powered Wireless Sensor Device for Machine Conditioning

ERIK ALMBRATT

RAKSHITHA BYADARAHALLI MADHUSUDHAN

UNIVERSITY OF GOTHENBURG

CHALMERS
UNIVERSITY OF TECHNOLOGY

Department of Computer Science and Engineering
Chalmers University of Technology
University of Gothenburg
Gothenburg, Sweden 2022

A Vibration-Powered Wireless Sensor Device for Machine Conditioning
ERIK ALMBRATT
RAKSHITHA BYADARAHALLI MADHUSUDHAN

Supervisor: Lena Petersson, Department of Computer Science and Engineering
Company advisors: Carina Engström and Paulina Eriksson, QRTECH
Examiner: Per Larsson-Edefors, Department of Computer Science and Engineering

Master's Thesis 2022
Department of Computer Science and Engineering
Chalmers University of Technology and University of Gothenburg
SE-412 96 Gothenburg
Telephone +46 31 772 1000

Cover: Grey scale plot of the power measurement results described in Section 5.1.

Typeset in LaTeX
Gothenburg, Sweden 2022

A Vibration-Powered Wireless Sensor Device for Machine Conditioning
ERIK ALMBRATT
RAKSHITHA BYADARAHALLI MADUSUDHAN
Department of Computer Science and Engineering
Chalmers University of Technology and University of Gothenburg

Abstract

Preventive maintenance is commonly accepted as an economical solution to prevent production stops. Machine conditioning may offer data, allowing a reduced frequency of maintenance. However, these machine conditioning sensors have to be maintained themselves, reducing users' confidence in the data. It may also make machine conditioning monitoring economically infeasible in some applications.

Vibration-based energy harvesting may provide a reliable and, most importantly, low maintenance energy source for such machine conditioning sensors. In this project we designed and evaluated the implementation of a vibration-logging wireless sensor device, transmitting over Bluetooth Low Energy 5, and powered by a commercially available electrodynamic vibration generator.

The results show that it is reasonable to expect a usable power output of around 0.1 to 6 mW, greatly depending on the vibration source. This amount of power enables microcontroller-based designs to operate indefinitely. However, the technology is limited by the low bandwidth of contemporary generators, making vibration-based energy harvesting difficult to implement. While vibration-based energy harvesting shows promise, it requires thorough investigations to be able to conclude whether an application is suitable for the technology.

Keywords: Machine Conditioning, Predictive Maintenance, Energy Harvesting, Wireless Sensor Network, WSN

Acknowledgements

First and foremost, we would like to express our gratitude to Martin Dermark, Manager Power Solutions, for providing us with the chance to complete this master's thesis at QRTECH. We appreciate the help and direction provided by our QRTECH supervisors, Carina Engström and Paulina Eriksson, who also took the time to address our questions throughout the thesis process.

We would like to express our gratitude to Lena Peterson, our academic supervisor at Chalmers University, who provided us with continuous input and guidance during the report writing process. We also would like to thank our examiner Per Larsson-Edefors for his guidance and feedback on this thesis.

Erik Almbratt, Gothenburg, October 2022
Rakshitha Byadarahalli Madhusudhan, Gothenburg, October 2022

Contents

List of Acronyms

6LoWPAN	IPv6 over Low-Power Wireless Personal Area Networks.
BLE	Bluetooth Low Energy.
DUT	Device Under Test.
EHC	Energy Harvesting Circuit.
EHM	Energy Harvesting Module.
IC	Integrated Circuit.
IEEE	Institute of Electrical and Electronics Engineers.
IOT	Internet of Things.
IP	Internet Protocol.
MCU	Microcontroller Unit.
MEMS	Micro-electromechanical systems.
PMIC	Power Management IC.
PSU	Power Supply Unit.
PZT	Lead Zirconate Titanate.
RFC	Request for Comments.
RMS	Root Mean Square.
SHM	Structural Health Monitoring.
WSN	Wireless Sensor Network.

1

Introduction

In production environments, downtime can become very costly. Machine conditioning methods predict machine failures, allowing companies to avoid production stops by preventively scheduling maintenance to be performed as soon as the symptoms are detected. Machine conditioning products are already widely available commercially [1–6] and this thesis presents the design and implementation of such an evaluation prototype, while employing energy harvesting to improve reliability.

For machine conditioning to be effective, sensor devices have to be extraordinarily reliable. Energy storage elements are a weak point in this regard, as they have to be replaced regularly. It is therefore promising to employ energy-harvesting techniques on such sensor devices to improve their reliability and life span and reduce the effort required to maintain them. These benefits are more significant in hazardous environments, where battery replacements are difficult, or impractical [7].

1.1 Project Aim and Approach

The aim of this project is to develop and evaluate a wireless sensor device powered by vibration-based energy harvesting intended for use in machine condition monitoring. The device measures vibration and temperature data, which are then sent to a database. The focus is on evaluating vibration-based energy harvesting and low-power design. There are three goals that are addressed in this project: implementing a vibration-based energy harvesting system, designing and developing a wireless sensor device, and visualization of the collected sensor data.

The device is split into the power supply unit (PSU) and the sensor board, as illustrated in Figure 1.1. This allows for separate evaluation but is not reasonable in a design intended for production.

The function of the PSU will be evaluated using a custom test rig, which agitates the device at varying acceleration and frequency. Generated and consumed power will be measured to create frequency-dependent graphs. Allowing us to estimate whether the device will be able to operate indefinitely by using the results from the test rig's measurements. The test rig's data will then be combined with application-specific vibration estimations from literature [7].

The project's goals and objectives are listed in Table 1.1 in order of decreasing priority. While only Goal 1, the energy harvesting part was finished, some of the sensor devices from Goal 2 are also described. However, the results are all based on vibration-based energy harvesting.

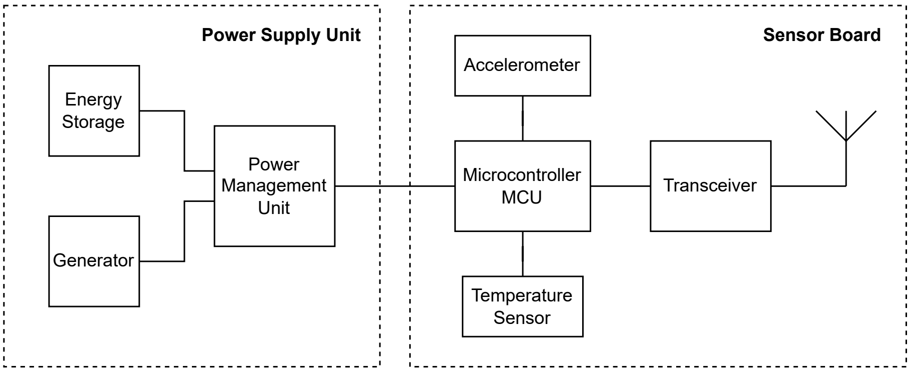

Figure 1.1: Overview of the sensor device.

Table 1.1: The project's goals and objectives with decreasing priority. The green tasks were completed. The yellow tasks were partly completed.

Goals		Objectives
Goal 1: Implement Vibration-based Energy Harvesting	1.1	Investigate available generators. Acquire a generator.
	1.2	Build a test-rig to measure the generator's efficiency.
	1.3	Measure the generator's efficiency.
	1.4	Design a power supply unit (PSU). Including energy storage and voltage conversion.
	1.5	Measure the PSU's efficiency.
Goal 2: Design a Wireless Sensor Device	2.1	Investigate low-power wireless network techniques. Choose a network technology.
	2.2	Investigate low-power design techniques. Choose an MCU and radio transmitter.
	2.3	Design the sensor device. Including accelerometer and temperature sensors.
	2.4	Develop minimal viable software for the MCU. Take sensor readings and transmit.
	2.5	Measure the sensor device's power consumption.
Goal 3: Visualize Sensor Data	3.1	Investigate IoT and data visualization software solutions. Choose a software stack.
	3.2	Store sensor data in a database.
	3.3	Visualize sensor data with some graphing software.

1.2 Related Work

Machine condition monitoring has been the topic of interest for many researchers and companies. Recently, research has been performed to use a wireless sensor network (WSN) to make the machine condition monitoring wireless while powering the WSN by waste energy in the machine's environment. One such study was performed by Escobedo et al. [8], who produced the first printed flexible tag for gas concentration monitoring in sealed environments. The tag was designed to be small, low cost, have a low power consumption and be powered by energy harvesting. The tag was able to operate under artificial light, powered by two small solar cells. However, it was concluded that continued work was required, as the artificial light was not enough to power the WSN.

Various parameters are used to measure the condition of a machine, such as a temperature, vibration, current speed, etc. One use-case was demonstrated by Discenzo et al. [9] where they used pressure and moisture sensors to monitor the condition of a fluid pump. They used a wireless sensor, which was powered using a piezoelectric generator.

Structural health monitoring (SHM) is a technique that monitor the health condition of infrastructures. SHM and machine condition monitoring are similar since both techniques monitor the condition of machines and infrastructure. Machines and infrastructure all wear out with time due to their operation as well as the environmental conditions. Park et al. [10] have studied SHM on civil, aerospace, and mechanical infrastructure. They measured the acceleration using an accelerometer, and a piezoelectric generator was used for energy harvesting. However, other researchers like Ha and Chang [11] investigated SHM using a Lamb-wave-based SHM system. Lamb waves are elastic waves that have particle motion in the plane, including the direction of wave propagation and the plane normal. These waves were first explained by Horace Lamb [11]. They concluded that using piezoelectric Lamb-wave-based SHMs, the overall power needed is significantly greater than the existing energy harvesting capabilities.

There exist many products that measure vibrations for machine conditioning. We discovered Broadsens [2], Treon [3], Perpetuum [4], and ReVibe [1] during our pre-study. Out of those, Perpetuum and ReVibe use vibration-based energy harvesting. The information we could find is summarized in Table 1.2.

Table 1.2: Review of some IoT machine conditioning products.

	Broadsens	**Treon**	**Perpetuum**	**ReVibe Connect**
Battery lifetime	Up to 5 years 1200 mA h, 3.6 V Non-rechargeable (0.5 year)	Up to 6 years 3.6 V Non-rechargeable (est. 3 years)	Indefinite "designed to work for 20 years"	Indefinite
Power consumption	Idle: ~7 µW DAQ & transm.: ~660 µW @ 3.3 V	-	-	-
Gateway-sensor network	2.4 GHz BLE 5.0 No Mesh	2.4 GHz BLE / Wirepas Mesh	-	2.4 GHz BLE
Sensor transmission range	≥300 m open space	-	-	-
Sample rate	Temp: Every 5 s Acc.: 50 Hz - 25.6 kHz	Default: Every 15 min Acc.: 10 Hz - 6.3 kHz FFT resolution: 1 Hz/bin	Every 5 min FFT every 6 h	-
Dimensions	34 x 31 mm Weight: 45 g	78.5 x 28 mm Weight: 129 g	65 x 87 mm	-
Environmental	−40 °C to 85 °C, IP67	−40 °C to 85 °C, IP67	−40 °C to 85 °C	IP69
Mounting	M6 Screw, alt. epoxy	M8 bolt	Thru-hole M6 bolt	-

Comparing the different products, it is clear that there exists variability when it comes to battery life and sample rate. However, the products are similar in their use of 3.6 V non-rechargeable lithium batteries. They are also similar in their choice of network, where all seem to use an 2.4 GHz based wireless network, and primarily Bluetooth Low Energy (BLE) 5.

1.3 Outline

This thesis is structured as follows: Chapter 2 explains in detail the fundamental concepts of the energy harvesting system and various related techniques. It also explains the importance of machine condition monitoring and provides a brief introduction to wireless networks that can be used for wireless communication. The design choice for implementing the energy harvesting system and the basic mechanical design are introduced in Chapter 3. Chapter 4 describes the test rig setup and how the measurement was taken using the test rig. The results gathered in this project are discussed in Chapter 5. Chapter 6 contains a short discussion on this project. This thesis is concluded in Chapter 7.

2

Technical Background

This chapter discusses machine condition monitoring and introduces the concept of energy harvesting systems and different types of energy harvesting technologies. This chapter also discusses various energy harvesting generators and wireless networks supported by commercial products.

2.1 Machine Conditioning

The condition of mechanical machinery may be estimated using many parameters such as temperature, vibration, humidity, oil samples, or power consumption [12]. To limit the project's scope, we will not delve deep into the theory or the algorithms required for practical machine conditioning. Instead, we will present an example of a self-powered platform for generic data logging. The presented hardware will log vibration and temperature data.

Out of these two parameters, vibration data are the most difficult to capture due to the large amounts of data involved. Vibration frequencies can imply mechanical failure in a very broad spectrum [12], leading to very large sample sizes that either have to be transmitted or processed. Unbalance, misalignment, or general looseness in machinery can be detected at low frequencies, between single Hertz to many kilohertz [12]. However, gear-boxes and bearings can often fail at frequencies over 50 kHz [12]. These frequencies are outside the capability of modern capacitive-MEMS accelerometers [13–15], such as those found in mobile phones, which mostly only sample at a few kilohertz. While other accelerometer technologies capable of measuring higher frequencies exist, these will not be covered in this project.

2.2 Energy Harvesting and Techniques

The basic concept of energy harvesting is the conversion from some other energy form to electrical energy that can be stored in a battery or a capacitor or can be used directly. A typical energy-harvesting system requires an energy source and an energy storage device as its minimum requirements. Energy harvesting plays an important role in condition monitoring where conversion of power in milliwatts or microwatts is possible. If energy-harvesting technology is adapted to condition monitoring of a machine, then the machine can be maintenance-free [16]. The need for energy harvesting becomes even more important when replacing or recharging the machine's batteries becomes costly and difficult.

Table 2.1 shows the power densities for various energy sources. When under the same condition, power density remains constant over time. In an energy-storage system, a leakage current is unavoidable. In industrial use, a typical energy density output has a power density of 100 µW/cm^2. In Table 2.1 "Human" refers to the application of wearable technology such as in thermoelectric-based watches or electronic foot bracelets.

Table 2.1: Power density of different energy sources [7].

Energy Source	**Type of Energy**	**Harvested Power [µW/cm^2]**
Human	Vibration/ Motion	4
Industry		100
Human	Temperature Difference	25
Industry		1000 − 10000
Indoor	Light	10
Outdoor		10000
GSM	RF	0.1
WiFi		1

Different forms of external sources can be converted into energy, e.g., solar, vibration, thermoelectric, and radio frequency. All these different types of energy-harvesting techniques are explained briA thermoelectric energy-harvesting technique converts temperature into electrical energy. The amount of power extracted is much lower than the heat flow. This is due to the low efficiency of the material [17]. The thermoelectric-based energy harvesting is generally used in wristwatches. In this case, the body heat is converted into electrical power. It is one of the best alternatives to use by reducing the necessity of replacing the battery used in electronic wristwatches. Mainly two companies have built such thermoelectric wristwatches: Citizen and Seiko [17] briefly in this section.

2.2.1 Solar Energy

Harvesting techniques based on solar energy convert light energy into electrical energy. It is mainly used outdoors since solar energy is available during the day. The power density of a commercially available photo-voltaic cell is 1.5 mW/cm^2, and it has 15% efficiency [18]. The solar-based energy harvesting technique is cost-effective since the collected energy during the day can be stored for usage. It provides more energy than vibration, thermoelectric, or RF, as shown in Table 2.1. However, it is not a feasible solution in dark environments or when the panel becomes dirty.

2.2.2 Thermoelectric Energy

A thermoelectric energy-harvesting technique converts temperature into electrical energy. Energy can be converted efficiently through temperature differences, while power can be generated through heat flow. Although large heat flows can be achieved, the extractable power is low due to low Carnot and material efficiencies [17]. A thermoelectric-based energy harvesting system is generally used in wristwatches. In this case, the body heat is converted into electrical power. By reducing the need to replace the battery in electronic wristwatches, it is one of the most viable alternatives. These thermoelectric wristwatches are mainly manufactured by Citizen and Seiko [17].

2.2.3 Radio Frequency Energy

This type of energy harvesting technique usually converts radio frequency signals in the surrounding environment into electrical power. These signals can be from TV, WiFi, cellular networks, etc. A power of 60 µW was generated from the antenna with the TV towers placed at a distance of 4.1 km away from the research lab by researchers at Intel [19].

2.2.4 Vibration Energy

The vibration-based energy is produced from converting the vibration or movements of the object into electrical energy. In vibration-based energy harvesting, the source and the resonant vibrations must match to generate power efficiently. Even a small variation in the source vibration will result in a significant reduction in output power [20]. Therefore, the tuning should be done by the manufacturer based on the intended application in which the device will be used. The vibration-based energy transducers are classified into electrostatic, piezoelectric, and electromagnetic.

In any vibration-based energy harvesting technique, frequency is a significant parameter. This is because the energy harvesting generator's output power is frequency dependent; this can be observed in one of the generator datasheet [21]. The bandwidth for the generators is defined between the points of 50% of the peak power values. The vibration-based generators are limited in bandwidth since with increase in the bandwidth the damping increases and the power output of the device decreases [7]. Further discussion on the bandwidth of different generators is provided in Section 3.1.2. Table 2.2 shows the frequency and acceleration values for various vibration sources. The peak acceleration values mentioned in this table are converted from $\mathrm{m/s^2}$ to g where $1\,\mathrm{g} \approx 9.8\,\mathrm{m/s^2}$.

Electrostatic

These electrostatic harvesters work with capacitive devices. When vibration energy is applied to the parallel plates, the area of the plate changes, or the distance between the plates changes. A 5 m vibration at a resonance frequency of 980 Hz might experimentally yield 1 W [22].

Table 2.2: Examples of some vibration sources. Taken from [7, Tab. 2.1].

Vibration source	**Peak acceleration** [g]	**Frequency** [Hz]
Car engine compartment	1.2	200
Base of 3-axis machine tool	1	70
Car instrument panel	0.3	13
Wooden deck with people walking	0.1	385
Window next to busy road	0.07	100
Washing machine	0.05	109
Refrigerator	0.01	240

Piezoelectric

Energy is generated from mechanical stress or movement using a piezoelectric transducer. The piezoelectric harvester uses different materials depending on the application. The most commonly used piezoelectric transducer is lead zirconate titanate (PZT) [23]. PZT is one of the most cost-effective and commercially available piezoelectric materials. One of the drawbacks of using a piezoelectric harvester is that it deteriorates over time. It might not be the ideal choice when harvesting energy for a longer period compared to electromagnetic transducer [24].

Electromagnetic

In the case of electromagnetic transducers, it work on the principle of electrical induction. It produces energy from a magnetic flux in the coil [25]. An electromagnetic transducer can work with larger bandwidth and relatively larger vibration than electrostatic [7]. The advantage of using an electromagnetic transducer is that it can modulate damping electrically to reduce impact when subjected to strong vibrations. The electromagnetic generator has to match the dominant frequency by tuning to a specific resonant vibration frequency.

2.2.5 Energy Harvesting ICs

Along with the energy harvesting generator, an energy management unit is called the energy harvesting IC. These integrated circuits are used to support and manage vibration-based transducers. The purpose of this IC is to facilitate the storage of energy from available resources. It assists in the discharge of stored energy when it is needed.

The energy harvesting IC will also help protect and maintain the regulation of charges to the energy storage element, like a battery or capacitor. This IC will act as a voltage regulator, which would not allow any damage to the battery or capacitor when there is a large current flow or load present in the system. In an energy harvesting system, the amount of current present is very small, so a simple voltage regulator could be sufficient. The advantage of using an energy harvesting IC is that it can help in monitoring the remaining charge in the battery [7].

2.3 Energy Storage Device

When electronic devices cannot produce enough power on their own and need to power an external device, energy storage devices are used to deliver the current. These energy storage devices capture energy, store it, and then deliver it to the device as needed. When the device demands more current, it can additionally supply the stored energy. Supercapacitors and batteries are the only two forms of energy storage devices.

Rechargeable batteries are available in the market in different sizes, spaces, and chemical compositions. It is usually available at a lower cost. The life of the battery starts to decrease when the discharging of the energy happens. The batteries continuously discharge to the energy harvesting device and also recharge themselves back [7].

A typical supercapacitor is very similar to a general capacitor. It is structured with an electric double layer [7]. Supercapacitors have very high leakage and high-temperature degradation, which may not be suitable for some applications. These supercapacitors can generally produce a current of 10 µA at a voltage of 2.5 V with a capacitance of 1 F [26].

2.4 Wireless Networks

As the name suggests, wireless networks are used in communication without the problem of using cables and wires. One of the major reasons for using a wireless network is portability. In condition monitoring, any machine would require a significant number of wires to transfer the data. An efficient solution to overcome such a drawback is to use a wireless sensor network (WSN). By using a WSN, the installation cost can be reduced. It also provides high flexibility.Various solutions were available when investigating the wireless network technology, and the comparison of these networks is shown in detail in Table 2.3.

Table 2.3 is taken from Tang et al. [16], which provides an efficient comparison of short-range wireless networks for energy-harvesting-powered machine conditioning devices. The table has then been complemented with information about BLE 5.

Table 2.3: Review of network technologies.

Technology	**Transmission Rate** [bps][1]	**Transmission Distance**	**Power Consumption**			**Features**
			Sleep [µW]	**Transmit** [mW]	**Receive** [mW]	
Low power Wi-Fi (802.11g)	54 M	1 km	300	350	270	High speed, high power consumption and high reliability.
BLE 5 [27–29]	2 M	Up to 200 m	4.29	54.12	42.57	High speed, long distance, wide bandwidth, ultra-low power consumption and high compatibility.
BLE 4.2	1 M	Up to 100 m. Normally operate within 10 m.	8	60	53	Low power consumption, low cost, high security and low latency.
Zigbee[2]	250 k	10 to 100 m	4	72	84	Low power consumption, low cost, low complexity and self-organization.

The table is based on [16, Tab. 1].
[1] Within immediate range. The achievable transmission rate at the rated transmission distance is drastically lower [27].
[2] Zigbee is based on the IEEE 802.15.4 MAC-PHY [30]. Other technologies such as WirelessHART or Miwi, which use IEEE 802.15.4 as well, have similar performance.
[3] BLE 5 power calulations are based on the nRF52840 chip with an supply voltage of 3.3 V [28]. Radio transmitting @ 8 dBm output power.

3

Implementation

In this chapter, the design choices for implementing the energy harvesting system are discussed, including the choice of the energy harvesting technique, the type of generator used, and the choice of the network gateway.

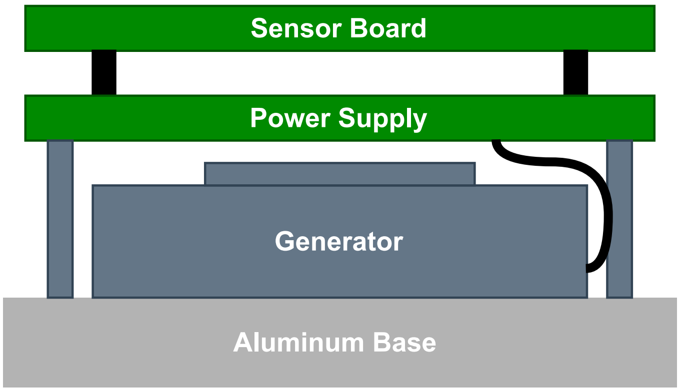

Figure 3.1: Mechanical design concept of the device.

Before the implementation, the basic concept of how the mechanical device will be constructed is demonstrated in Figure 3.1. The mechanical design is constructed using a 3D-printed model made of plastic as the base, with the generator mounted on top using screws. The power supply shown in Figure 3.1 consists of the power PCB, which is mounted on top of the surface of the 3D model. The accelerometer will be placed close to the generator. The generator output will be connected to the PCB using a pin header.

This mechanical design was chosen to provide a rigid mounting for the generator.

3.1 Power Supply Unit

The power supply unit (PSU) consists of a power management unit, an energy harvesting generator, and an energy storage unit as shown in Figure 1.1. The requirements of the PSU implementation is tightly coupled to the sensor board's power consumption. These metrics are later evaluated in Section 5.4.

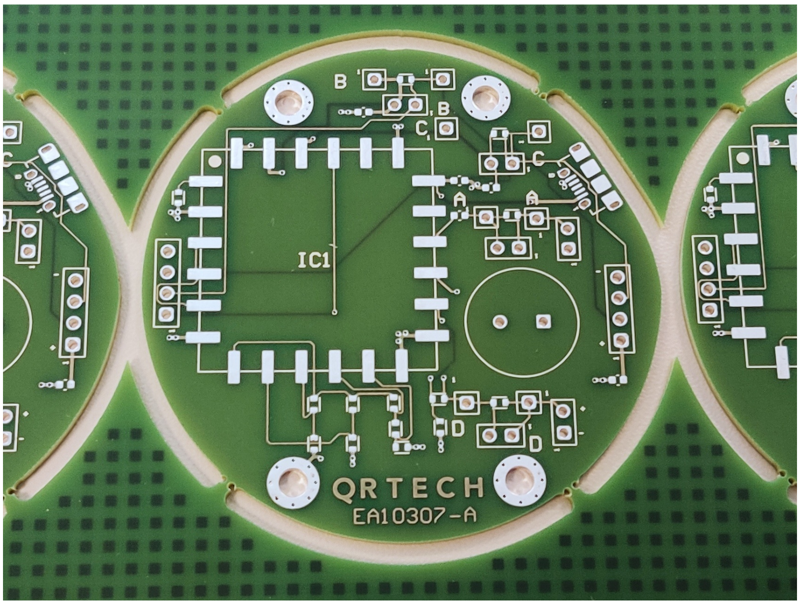

Figure 3.2: The unassembled, panelized PSU PCB.

3.1.1 Choice of Energy Harvesting Technique

There are different types of energy harvesting as mentioned in Section 2.2. Solar power may provide more energy but becomes useless in dark environments or when the panel becomes dirty. When it comes to thermoelectric harvesters, they are not reliable for machine conditioning since they produce less power compared to vibration harvesters. The use of large and space-consuming radio frequency antennas might not be an ideal choice in the case of machine condition monitoring. So, the best choice of energy harvesting technique is to use a vibration-based energy harvester. It is not prone to dirt and works well in any environment, i.e., indoors and outdoors. So, the first design choice is to use a vibration-based energy harvesting technique.

3.1.2 Choice of Energy Harvesting Generator

In Section 2.2.4 three different vibration-based energy harvesting techniques were mentioned. Among these three, piezoelectric and electromagnetic generators are a good choice for machine condition monitoring. One of the similarities between electromagnetic and piezoelectric is that they both have to match the dominant frequency by tuning to a specific resonant frequency. One of the main drawbacks of choosing a piezoelectric transducer is that they produce a very low power output compared to the electromagnetic vibration-based transducer. So, electromagnetic energy harvesting generators were the second design choice for our machine condition monitoring.

When investigating the energy harvesting generator, three generators were highlighted, which were from Xidas, Perpetuum and ReVibe. Perpetuum is an electromagnetic vibration-based transducer that was used in Yorkshire water plant in Blackburn. These generators usually produce vibration and have a larger frequency range. With 25 mg acceleration Perpetuum produces a power of 1 mW peak and with a bandwidth of 2 Hz [7].The generators from Perpetuum were used for condition monitoring with wireless sensor networks.

Table 3.1: Comparison of different energy harvesting generators. The values are taken from the manufacturers's website.

Generator	**Bandwidth** [Hz]	**Acceleration** [g]	**Power Output** [mW]
Xidas [21]	2.5	0.1	1
ReVibe [1]	5	0.1	4.5
Perpetuum [4]	2	0.1	10

All three generators work at an acceleration of 0.1 g. However, all three generators vary slightly in their bandwidth and a significant number in their output power. As the output power produced by these generators must be larger, the Perpetuum generator was the ideal choice. Perpetuum also has a fair bandwidth of 2 Hz. Even though the specification of ReVibe provides better bandwidth as well as better power output, and they assure to provide an output power of 4.5 mW with 0.1 g. Neither Perpetuum nor ReVibe´s generator was not available for purchase. Even with a lower output power of 1 mW with an acceleration of 0.1 g and bandwidth of 2.5 Hz Xidas transducer seems to be more practical and shows realistic data.

3.1.3 Choice of Energy Harvesting IC

The purpose of an energy harvesting IC is already mentioned in Section 2.2.5. There are several energy harvesting ICs present in the market, particularly for operating with electromagnetic-based transducers; some of them are LTC3331 by Analog [31], BQ25570 from Texas Instruments [32], and SPV1050 from ST Microelectronics [33]. For simplicity of our design choice, we chose the energy harvesting and power management module EHM-UNIV-1 from Xidas [34]. It will be easy to work with since the Xidas provides pre-calculated values for the configuration resistors required for the Vibration Energy Harvesting Generator (VEG). That way, we do not have to spend time characterizing the generator.

3.2 Sensor Board

The sensor board hosts the microcontroller, transceiver, and sensors, as shown in Figure 3.3. The interface to the power supply board consists of supply voltage (VSYS), battery voltage (VBAT) for charge measurement, and power good (PGOOD) which signals whether the power supply is ready for operation. The board is based around the nRF52840 Dongle [35], chosen for the nRF52840s' good Bluetooth Low Energy (BLE) 5 support and thorough documentation. The decision to use BLE 5 is described in this Section. A picture of the nRF52840 Dongle is shown in Figure 3.4.

The board is fitted with ST's IIS3DWB accelerometer, chosen for its high output data rate (ODR) of 26.667 kHz, which significantly outperforms other available

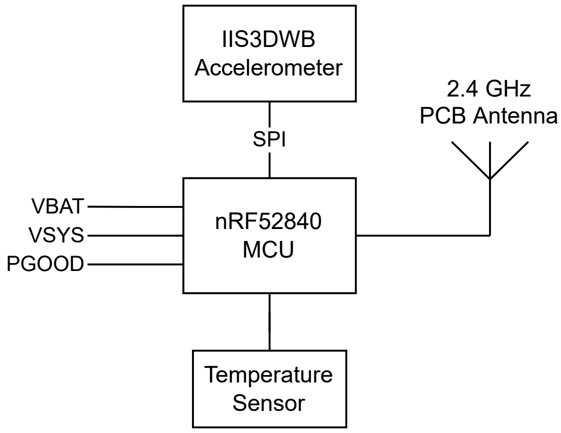

Figure 3.3: Sensor board block diagram.

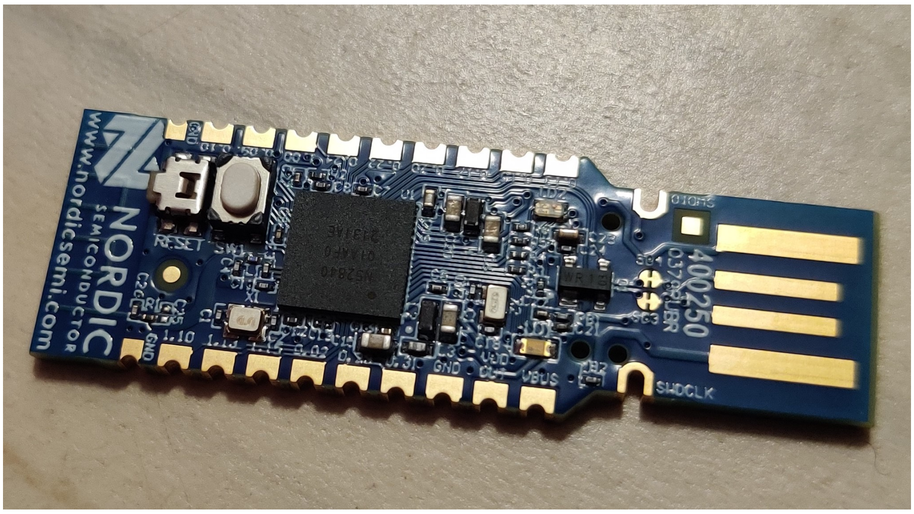

Figure 3.4: The nRF52840 Dongle, which the sensor board is based on.

accelerometers. Using this accelerometer, our design would provide the same acceleration measurement features as other similar commercially available machine conditioning devices [3]. The reason to use a capacitive-MEMS accelerometer, in contrast to, for example, piezoelectric accelerometers, was to keep design complexity down.

The choice of network technology was previously investigated and compiled in Table 2.3. This investigation made it clear that 2.4 GHz-based networks are used by most manufacturers in the vibration machine-conditioning space [1–3, 5]. Several companies used BLE 5, but BLE 4, IEEE 802.15.4, and WiFi.

Tang et al. [16], who have done an extensive survey into the application of low-power machine conditioning, concluded that the amount of data required for acceleration measurements would require a high-transmission speed network to be the most power efficient. This explains the common use of 2.4 GHz networks. Our application would benefit from a longer range than traditional 2.4 GHz networks. In this regard, BLE 5's specification outperforms BLE 4 and IEEE 802.15.4.

BLE 5 fulfills the project's requirements at reasonably low power consumption. BLE

5's specification outperforms BLE 4 and IEEE 802.15.4 regarding range while not consuming much more power [16, 27, 28]. This, in combination with BLE 5's higher data rate, resulted in us choosing BLE 5 for the design.

3.3 Network Gateway

The function of the network gateway is to transfer data between BLE 5 and the internet. An overview of the hardware is shown in Figure 3.5. The choice of network modem can be fulfilled by a broad range of products that are available commercially. We used a Raspberry Pi 2, as we had one at hand, with Ethernet and an ASUS USB-BT500 Bluetooth 5 dongle.

Neither Bluetooth nor the rivaling technology IEEE 802.15.4 has native support for the Internet Protocol (IP) [27]. Thus, additional software has to be added to enable IoT applications. This could be done over Bluetooth's Generic Attribute Profile (GATT) and be implemented in the application layer, which is the traditional approach. The downside of implementing the conversion manually in the application layer is that every data transfer has to be recognized by the sensor device, the network gateway, and the back-end server. This requires three code bases, all of which have to be maintained. It is also very rigid, as the gateway has to be re-programmed for every new feature in the sensor device.

An alternative is IPv6 over low-power wireless personal area networks (6LoWPAN) over BLE, as specified in RFC 7668 [36]. 6LoWPAN acts as an adaptive layer between the link layer and the IP network layer, allowing IP traffic directly between the sensor device and the back-end server. The major downside to 6LoWPAN is the large size of IP headers. Header compression is utilized to maximize the payload size. However, 6LoWPAN will not be ideal in a low-power implementation but will allow for more complex and flexible network architecture. This is implemented in the design.

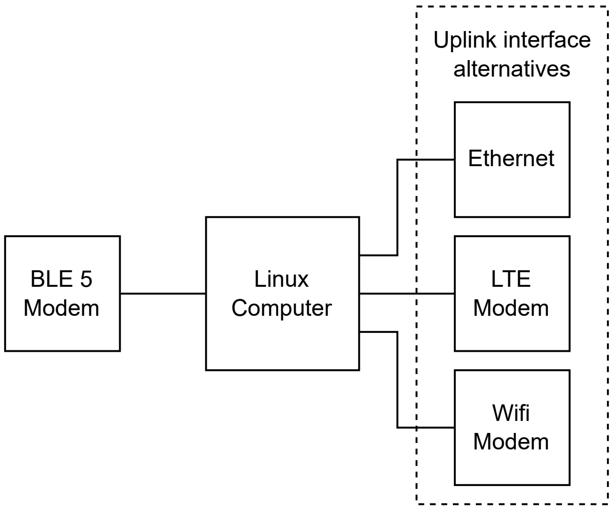

Figure 3.5: Network gateway block diagram. Where an ASUS USB-BT500 is used as a BLE 5 modem. A Raspberry Pi 2 was used as a Linux computer.

4

Evaluation

This chapter describes the test rig implemented to collect the measurement data for analysis of the system. It describes how the measurements were taken and what parameters were measured during the project.

4.1 Vibration Test Rig

A vibration test rig is required to excite the generator in a controlled manner. This would help us verify the Xidas generator's performance and energy harvesting circuit. There is equipment available in the market that generates the vibration required to excite the generator. It is called a model shaker or a vibration exciter. The generator's manufacturer, Xidas, has demonstrated [37] their vibration perpetual power pod using a shaker produced by The Modal Shop [38]. The shaker which was demonstrated would have been preferred, but due to the project's budget, we had to build our own vibration test rig.

Initially, the idea was to build a test rig with linear rails and motors. However, it was later realized that the mechanical backlash of the preliminary design would be more significant than the total travel. Another approach for a vibration test rig was described in Lithwhiler's [39] paper using a sub-woofer as the transducer. This setup was meant to be used for student laboratory work and is likely easy to implement. A sub-woofer cannot be assumed to be linear. However, paired with a quality accelerometer, it is possible to excite the DUT at a known frequency and amplitude. We decided to refer to [39] and implement the same vibration test setup for our project. We used the same components, like the accelerometer [40], and biasing circuit, which consisted of an LED, a capacitor, and BNC pins for connection to the oscilloscope. But, the only change was the speaker; we used an Edifier S330D sub-woofer with an integrated amplifier since it was already available in our lab.

For the vibration test measurements, we used a computer audio output, which would provide excitation sine wave signals, and to measure the reference acceleration, an accelerometer was used. The accelerometer output signal was measured using an oscilloscope. On the surface of the sub-woofer cone, the mechanical design setup, which includes a generator and a power PCB, mounted using hot glue. For stability and convenience, the accelerometer was glued close to the generator on the base of the 3D model. The power PCB and the generator were mounted on the 3D model using screws. There was an unbalance when the speaker was placed with the sub-woofer facing the top since the bottom of the speaker had switches and connection ports. So, wooden blocks were glued on all four sides of the speaker to ensure it had a uniform platform to get optimal power from the generator.

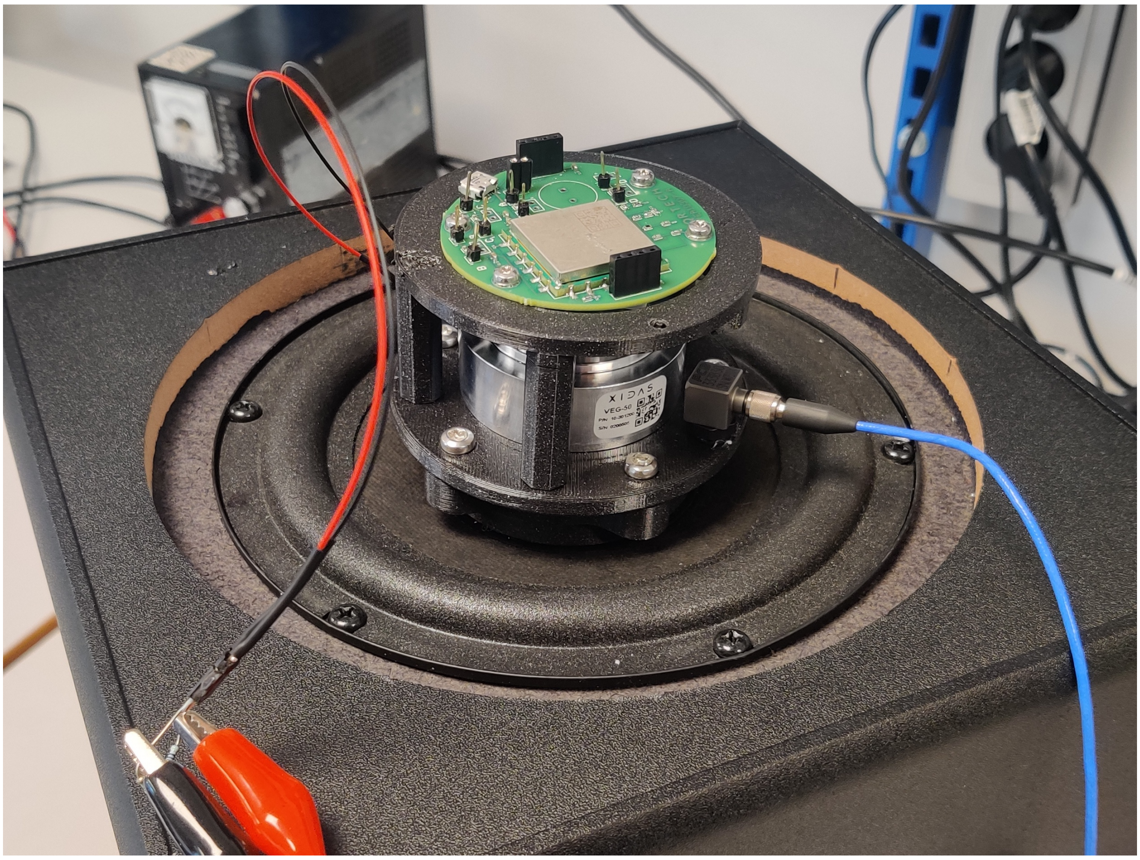

Figure 4.1: Test setup for measuring power over a 440 Ω resistor connected to a Xidas VP3 generator. An Edifier S330D sub-woofer was used to excite the generator. A 333B30 accelerometer [40] was used to verify the excitation amplitude.

4.2 Power Delivered to a Constant Load

The first test evaluated the generator's ability to produce power. In this test, the generator was completely disconnected from the energy harvesting module (EHM) and only connected to a fixed 440 Ω resistor, as illustrated in Figure 4.2. This test was set up to re-create the tests presented in the generator's datasheet [21]. The results would then tell whether the generators performed as expected or if there was some disparity between the measurements and the manufacturer's results. This could depend on differences in the test setup or the production of the generator.

The voltage over the resistor and the accelerometer's output was measured with a Rigol DS1054Z oscilloscope. A pure sine wave, varying between 45 and 55 Hz would be fed into the sub-woofer. Then, the oscilloscope's "Measure All" function was used to read the RMS voltage of both signals. The vibration's amplitude was manually tuned by reading the accelerometer's output and manually adjusting the volume fed into the sub-woofer. Then, the resulting RMS voltage, measured over the resistor, was noted. The compiled result is shown in Section 5.1.

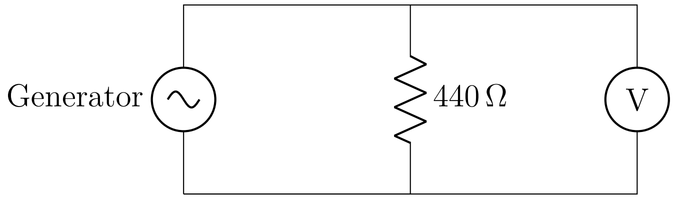

Figure 4.2: Power delivered to a constant load.

4.3 Power Delivered to a Capacitor

To show that the generator, together with the EHM, would produce usable power, it was necessary to show that the assembly could charge a battery. The EHM can charge either a capacitor or a lithium battery, but a capacitor was preferred for this test as fully charging a lithium battery would have taken too much time. An 1000 µF electrolytic capacitor was connected to the EHM's VBAT pin, as illustrated in Figure 4.3.

The EHM was configured for an upper charging voltage of 4 V, set by resistors R_2 and R_3, and a lower charging voltage over 3.3 V, set by resistors R_4 and R_5. The schematic can be seen in Appendix A. If this upper charging voltage could be seen in the results, at least basic functionality could be assumed. During the test, the vibration's frequency was held constant, while the amplitude was varied. The accelerometer was read using an oscilloscope, just as described in Section 4.2 while a PicoScope 4824 USB oscilloscope was used to log the voltage over the capacitor. The compiled result is shown in Section 5.2.

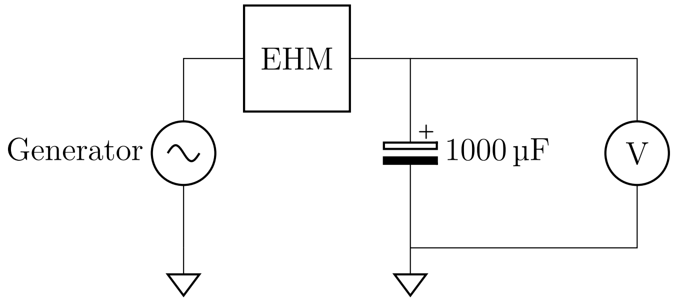

Figure 4.3: Power delivered to a capacitor through the energy harvesting module (EHM) with the capacitor connected to the EHM's VBAT pin.

4.4 Efficiency Measurements of the Energy Harvesting Module

To successfully estimate the allowable wake-up frequency[1], an efficiency factor has to be known. To measure this efficiency, the voltage and current were measured over

[1] I.e. how often the device can wake up, sample, and transmit data, as described in Section 5.4.

shunt resistors at the input and output of the EHM, as illustrated in Figure 4.4. Like the earlier tests, frequency and amplitude were varied and controlled with the accelerometer. Two Agilent U1232A multimeters were used to measure the voltage over the shunts to signal ground. An Agilent U1252B multimeter was used to measure the voltage over the input shunt resistor. The input and output powers were calculated, and the result is shown in Section 5.3.

The EHM is based on the ADP5091 power management unit. Thus, it is expected that the EHM's resulting efficiency would comply with the efficiency stated in ADP5091's datasheet [41]. Another reference is Xidas' power pod product VP3 [42], which consists of the same generator and EHM. Thus, the rated power could be compared to the generator's datasheet to estimate efficiency.

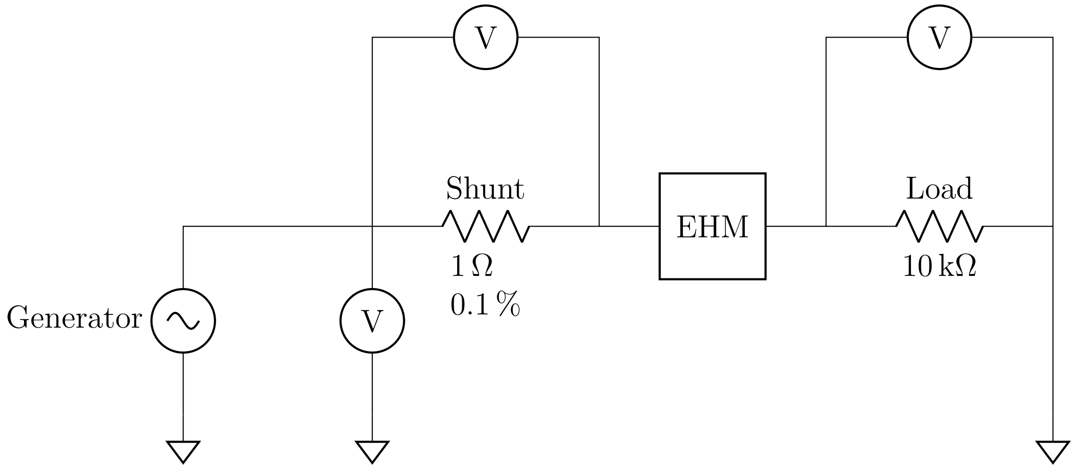

Figure 4.4: Efficiency measurements of the energy harvesting module (EHM) with the load connected to the EHM's VSYS pin.

5

Results

In this chapter the results based on the test setup using a load and capacitor are discussed using graphs and tables. It also includes the efficiency test results of the Xidas generator used in the project.

5.1 Power Delivered to a Constant Load

Figure 5.1 visualizes the results of the measurement described in Section 4.2. It is evident, as the plot forms a steep peak, that the power output of the generator is strongly dependent on the frequency. This is also expected and reflects existing literature [7] and the generator's datasheet [21].

The result does differ in amplitude and center frequency. According to the datasheet, the generator should have a peak power of about 30 mW during an excitation of 0.5 g. However, the measurements only show about 18 mW. This is only 60 % of the expected power. The center frequency is expected to be precisely at 50 Hz but it is offset almost at 49 Hz, which is significant as the slope is so steep.

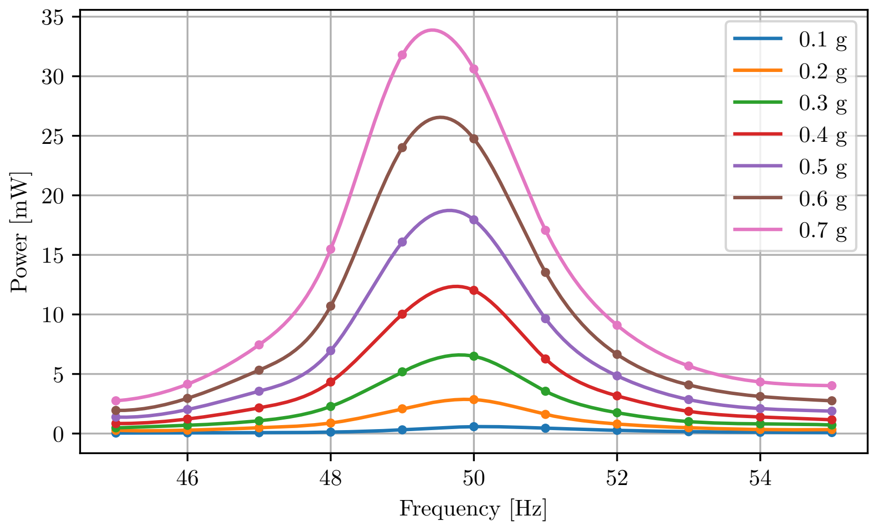

Figure 5.1: Measured power over a 440 Ω resistor connected to a Xidas VEG generator tuned for 50 Hz. The generator was excited with varying frequency and acceleration. The acceleration is measured in RMS g.

5.2 Power Delivered to a Capacitor

Figure 5.2 shows the measurement described in Section 4.3. It shows that the capacitor is successfully being charged by the EHM. It also shows that an increase in the excitation's amplitude reflects in an increase in the rate at which the capacitor is charged. The upper charge limit, set to 4 V, is somewhat overshot. But, it does seem to regulate correctly, and the slight difference in target voltage could simply be due to the tolerance of the configuration resistors.

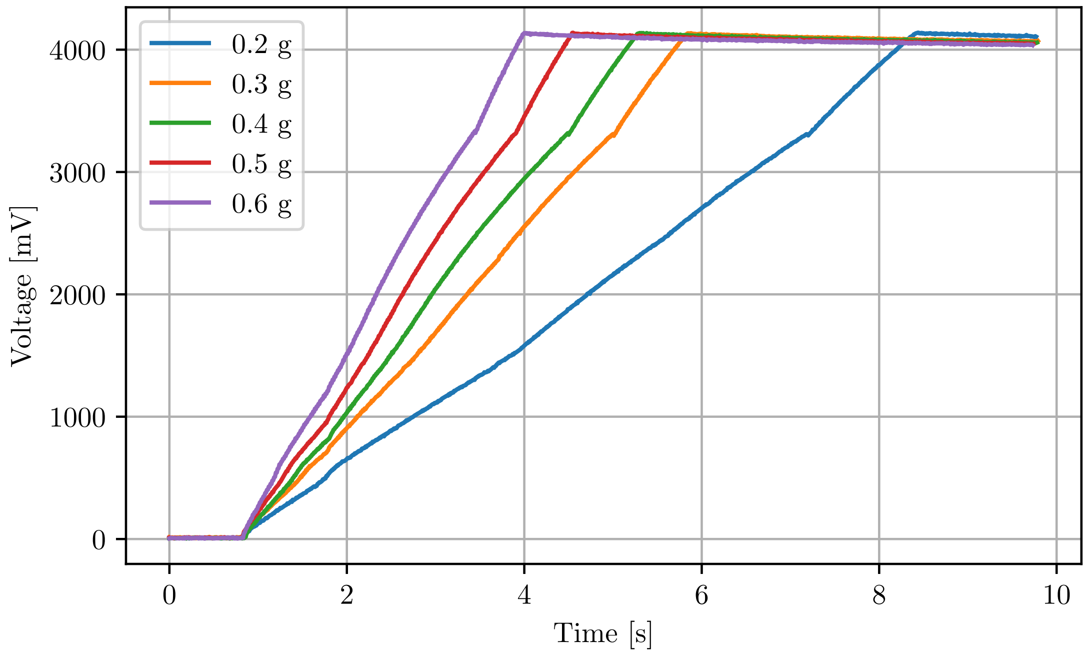

Figure 5.2: Voltage measured over a 1000 µF capacitor connected to the energy harvesting module's VBAT. The device was excited at 50 Hz with varying amplitude.

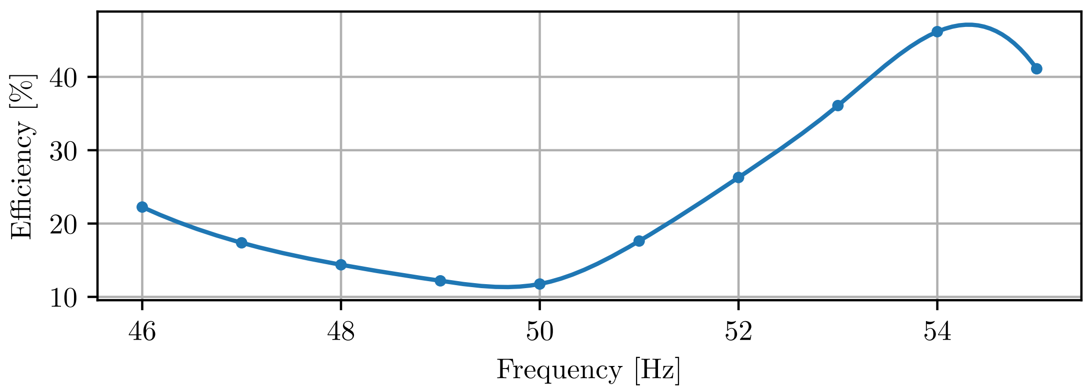

Figure 5.3: Efficiency of the EHM with varying frequency. Constant amplitude of 0.6 g. 10 kΩ load.

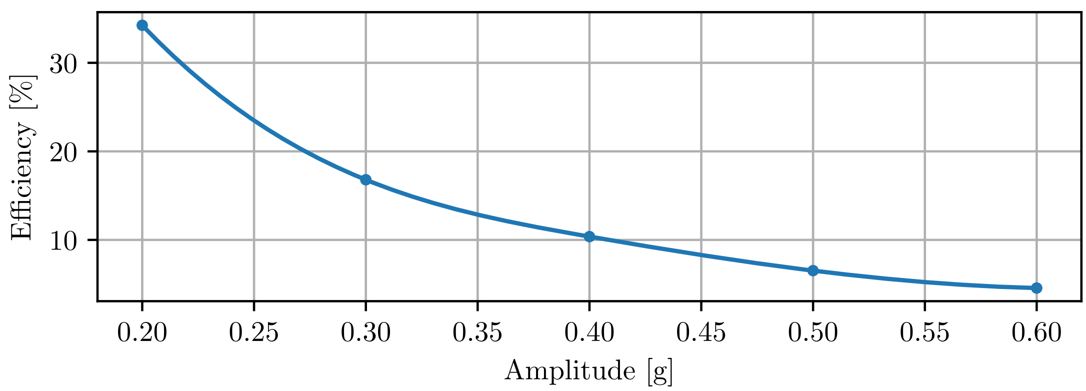

Figure 5.4: Efficiency of the EHM with varying amplitude. Constant frequency of 50 Hz. 10 kΩ load.

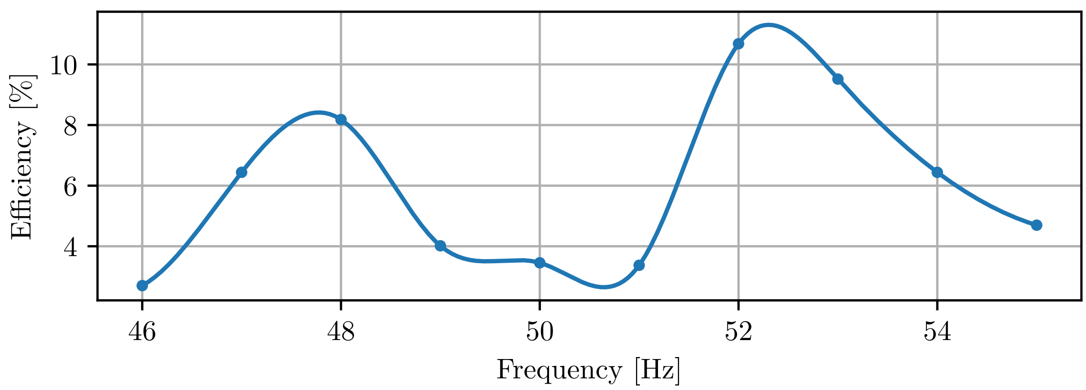

Figure 5.5: Efficiency of the EHM with varying frequency. Constant amplitude of 0.6 g. 1 kΩ load.

5.3 Efficiency Measurements of the Energy Harvesting Module

Figures 5.3, 5.4 and 5.5 show the result of the measurement described in Section 4.4. The resulting efficiency, in the range of 40 to 4 % could be reasonable, but the curves does not behave as we had expected. The efficiency of the ADP5091 chip, which the EHM is based on, increases with higher input voltages [41, Fig. 6]. Thus, it was expected that Figures 5.3 and 5.5, showing varying frequency, would follow the same form as Figure 5.1 and that Figure 5.4, showing varying amplitude, would linearly increase.

As we are not able to confidently explain these efficiency measurements, we will not use them in the following calculations.

5.4 Minimum Viable Wake-up Interval

Here an estimation of a viable wake-up pattern is made based on the previous power measurements. But, as the sensor board was not completed, the power draw had to be estimated. Nordic Semiconductor's Online Power Profiler for BLE [43] was used for this purpose.

Provided the FFT sample amount is 4096 samples of acceleration data, which is the maximum amount used by Treon [3], and that each sample consists of 16 bits [15], this would then result in $4096 \cdot 16\,\text{bits} = 8192\,\text{bytes}$ that would have to be transmitted. (This does not include any potential packet overhead.) This is much larger than the typical amount of data that would be transmitted over BLE, making all phases but the transmit (TX) phase negligible. Thus, only the phases when the antenna is active are taken into account. This information, taken from the Online Power Profiler is compiled in Table 5.1, yielding an average power consumption of about 30 mW.

Table 5.1: Average power consumption of nRF52840 during BLE transmission according to Nordic's Online Power Profiler for BLE [43]. Voltage: 3.3 V. Radio TX power: 8 dBm. PHY = 1 Mbps.

Phase	**Time** [µs]	**Current** [mA]	**Power** [mW]
Radio switch	150	3.3	10.89
Radio RX	88	6.1	20.13
Radio switch	140	3.5	11.55
Radio TX	296	15.1	49.83
Average		8.89	29.33

Alternative power estimations are listed in Appendix C. These may be more relevant, depending on application-specific conditions such as range and obstruction. They differ in the selected transmission speed (2 Mbps in contrast to 1 Mbps) and transmission power (4 dBm in contrast to 8 dBm).

The wake-up time will be dominated by two phases: the accelerometer sample phase, and the BLE transmission phase. To capture the 4096 samples with the IIS3DWB accelerometer, which operates at 26 kHz [15], this would take $4096/26\,\text{kHz} \approx 160\,\text{ms}$. Then, to transmit that data with a 1 Mbps transmission rate, this would take $8192\,\text{bytes}/1\,\text{Mbps} = 70\,\text{ms}$. This information is compiled into Table 5.2, assuming a constant power consumption of 40 mW.

Due to the inconclusive efficiency measurements, a rough estimate was formed by comparing the power output of the Xidas VP3 power pod, which contains the same generator, and the EHM. The peak values (at 50 Hz) were noted of both the VP3 and VEG generator and an efficiency was calculated as compiled in Table 5.3. Based on these measurements, a flat 20 % efficiency was assumed for the following calculations.

Finally, by combining the generator power measurements, MCU power consumption and EHM efficiency, viable wake-up intervals can be calculated. Simply divide the required energy per wake-up. This is compiled, with varying amplitude, in Table 5.4.

$$\text{Minimum viable wake-up interval} = \frac{\text{Consumed energy [W h]}}{\text{Generated power [W]} \cdot \text{Efficiency}}$$

Table 5.2: Estimated energy consumption per wake-up routine. Voltage: 3.3 V. Radio TX power: 8 dBm. PHY = 1 Mbps.

Phase	**Time** [ms]	**Power** [mW]	**Consumed energy** [µW h]
Sample	160	40[1]	1.78
Transmission	70	40	0.78
Total	231	80	2.56

[1] The sample power is likely more in the range of 20 mW as the antenna is not active in this phase. But, without data to support that, we will proceed with this estimation.

Table 5.3: Estimation of the energy harvesting module's efficiency. Based on the power measurements stated in the VP3 power pod's datasheet [42] and the VEG generator's datasheet [21].

Vibration amplitude[1][g]	**VP3** [mW]	**VEG** [mW]	**Efficiency** [%]
0.1	0.3	2.5	12
0.2	1.2	5	24
0.3	2.6	12	21.67
0.4	4.5	20	22.50
0.5	6.4	31	20.65

[1] At 50 Hz.

Table 5.4: The shortest wake-up interval possible, calculated from the previously measured power generation.

Vibration amplitude[1][g]	**Generated power** [mW]	**Usable power**[2] [mW]	**Minimum wake-up interval** [s]
0.1	0.6	0.12	76.80
0.2	2.9	0.58	15.89
0.3	6.5	1.3	7.09
0.4	12	2.4	3.84
0.5	18	3.6	2.56
0.6	25	5	1.84
0.7	31	6.2	1.49

[1] A 50 Hz sine wave. Generated power as shown in Figure 5.1.
[2] Assuming 20 % efficiency.

Further estimations can be made from Tang et al.'s [16, Tab. 2] estimated power figures. They provide transmission power and sleep power estimations for several BLE 5-based microcontrollers, among them Texas Instrument's CC2640R2F [44] and the nRF52840. Using this power data, the active times from Table 5.2 and assuming a usable generated power of 500 µW, the net energy over time of different active intervals is calculated. These are presented in Figures 5.6 and 5.7. In short, the CC2640 estimation agrees with the results presented in Table 5.4 while the nRF52840 estimation is more conservative.

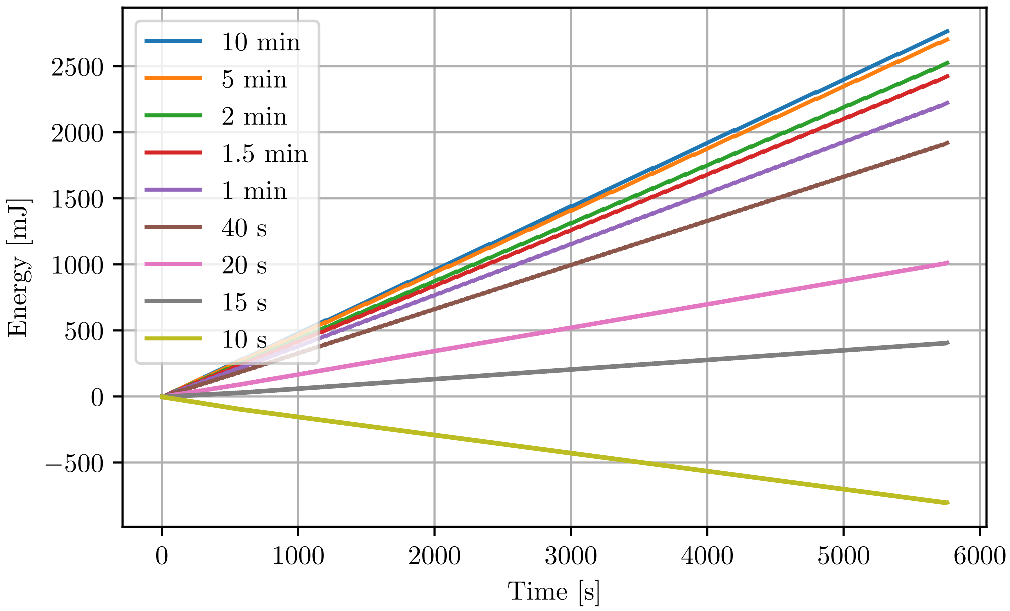

Figure 5.6: Calculated net energy of a CC2640 MCU with different wake-up intervals assuming 27.3 mW active power consumption, 9 µW sleep power consumption, 500 µW usable power generated, and 231 ms active time.

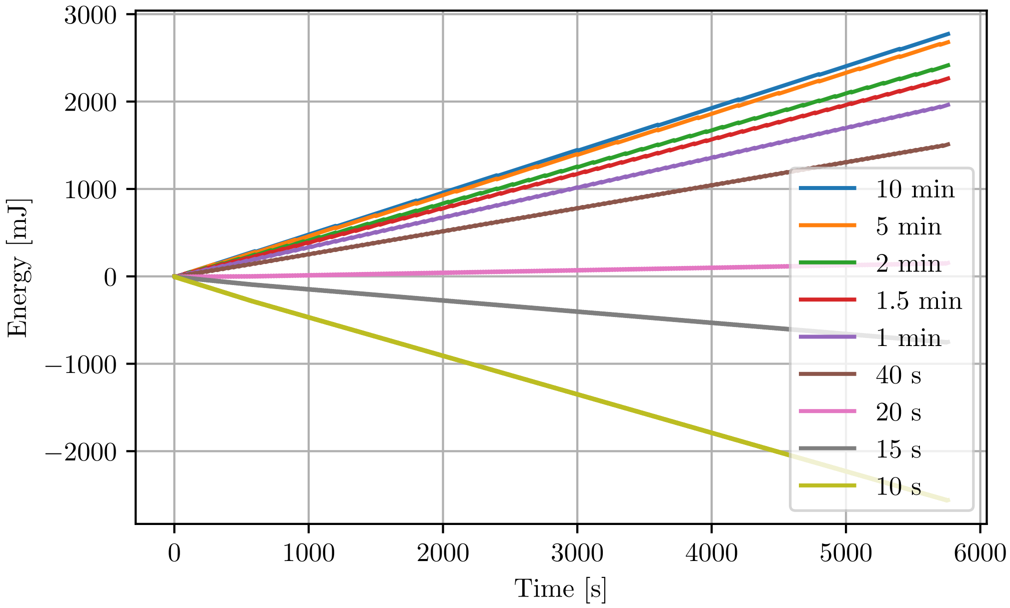

Figure 5.7: Calculated net energy of a nRF52840 MCU with different wake-up intervals assuming 40.8 mW active power consumption, 2.1 µW sleep power consumption, 500 µW usable power generated, and 231 ms active time.

6
Discussion

This chapter discusses the different aspects that might have influenced the results, potential improvement, and future work.

6.1 Xidas Generator

The Xidas generator was sensitive to over-excitation. The datasheet mentions that the maximum acceleration the generators can handle is 0.9 g which they were exposed to during the peaks. One of the generators was purposely exposed to an acceleration of 1 g. The generator had inconsistent measurements after the acceleration was set to 1 g and also had metallic sound at higher amplitudes. At the end of the project both the generators had the metallic sound at higher amplitude, indicating that the generator had been damaged.

The screws used to mount the generator were plastic, which is not ideal according to the datasheet. The datasheet recommends using zinc-coated or aluminum body screws to mount the generator. It was also recommended in the datasheet to use metallic plates as the surface to mount the generator, but a plastic 3D model was used in the project. This could have affected the measurement values. The use of adhesive glue in the generator's threaded location was recommended to maintain a good interface during the vibration in the Xidas datasheet. The test leads could weigh the device down, affecting the measurements due to the additional inertia. This could be seen on the accelerometer waveform when the test leads were not properly installed.

6.2 Test Rig

The mechanical part was mounted on the cone of the sub-woofer using hot glue, as mentioned in Section 4.1. When mounting, an excessive amount of glue was used, which made the mechanical part not placed exactly 90° to the speaker surface. This could also have affected the results taken with the test-rig setup.

The deviations in the results mentioned in Section 5.1 could be due to flaws in the test rig. For example, the measurements were taken with the test rig placed on a concrete floor. But, placing the rig on a wooden table would shift the center frequency almost a whole Hertz. This is likely due to a resonant frequency introduced by the tabletop. Many commercial vibration testers are made of cast steel or stiff material, while the sub-woofer is constructed from a chipboard.

The mounting consideration stated in the generator's datasheet [21] is specific that the generator should be mounted with metal screws, thread adhesive, and locking washers, neither of which was fulfilled in these tests. Due to a misorder, nylon screws had to be used.

6.3 Ethical Considerations

When used in real-world applications, the Xidas generators employed in the project would not be particularly dependable. This was seen in the test results with two identical generators, which showed signs of mechanical failure and altered electrical characteristics after the tests. Applications that require vibration-based energy harvesting likely also require a high level of dependability. A generator should be rugged enough to have a lifespan significantly longer than a battery. Otherwise, many applications, in other aspects suitable for vibration-based energy harvesting, may be better served by another technology. While Xidas' generator showed less reliability than expected, other manufacturers seem to provide higher levels of mechanical reliability. This can be seen in the generator's differing maximum acceleration ratings [1, 4, 21].

The electrodynamic generators are expensive, and the production of these generators is not sustainable at a very large scale due to the amount of materials required. They may, therefore, not be sustainable for many consumer applications.

Energy harvesting may be sustainable because it allows for using smaller or no batteries. As a result, smaller amounts of ethically sensitive materials, such as lithium, are used. However, materials are also required to produce the generators and energy harvesting circuitry. The use of rechargeable lithium-ion batteries used in the project has a downside. Recycling batteries is harmful to both the environment as well as humans.

7
Conclusion

This project set out to be a complete case study, implementing a vibration-powered IoT device in a practical context. The goal was to evaluate the viability of a contemporary vibration-generator solution and conclude whether the technology was viable and dependable. By the end of this project, we have confirmed what was already documented in the literature: Vibration-based energy harvesting is a viable energy source for low-power electronics when a well-defined vibration source exists.

The 'general' power source, capable of being mounted on any arbitrary vibrating equipment, which was envisioned before the project, is however, not viable. Instead, it is likely applicable to narrow, well-defined applications where reliability, low maintenance, and longevity are prioritized.

Our measurements show that our theoretical device would be able to record and transmit acceleration data for an 26 kHz FFT every two seconds, granted an acceleration of 0.6 g or more at the generator's tuned frequency.

However, we do not have any data about vibrations on specific machines. The data sets of machine vibrations we found either have too low sample rates or do not provide frequency data. These data sets are not helpful for our conclusion. But we can make some conclusions from the vibration data presented in Table 2.2.

From Table 5.4 we can see that a wake-up interval of just over a minute is viable with a resonant vibration amplitude of only 0.1 g. According to Table 2.2 0.1 g would be comparable to the amplitude resulting from a wooden deck being walked upon. So, the device would be able to operate from a subjectively 'low' amount of vibration. Any machine that vibrates significantly would likely be able to power the device by a good margin. However, this must be confirmed with real-world data, which was not done in this project.

The amplitude of vibrations is probably not the limiting factor. Instead, it is likely the frequency, as it is more difficult to predict. A rough estimation of the peak frequency can be made from a motor's rotational frequency and additional peaks multiplied with any eventual gearing. However, this peak frequency may easily be offset by a few Hertz from the mechanical structures on which the generator would be mounted. The generator's total bandwidth is very narrow at only around 3 Hz, and competitors' generators exhibit bandwidths between 1.6 and 4 Hz [1, 4]. So, a mispositioned generator could very likely result in the majority of the available energy being missed.

The generator's low bandwidth requires the designer of the system to measure the vibration's peak frequency at the specific place they plan to mount the generator.

This makes it challenging to know beforehand whether or not vibration-based energy harvesting is a viable technology for a specific application. The technology requires prior investment in vibration measurement equipment. This will likely hinder the future adoption of the technology.

But to reiterate, the results presented in Table 5.4 did show that powering a contemporary microcontroller from a commercially available electrodynamic vibration generator is feasible. It is, however, not necessarily practical as it imposes strict limitations on sampling frequencies and the device's placement.

Bibliography

[1] Revibe Energy AB. (2021, Dec) Revibe energy. Accessed on 2021-12-03. [Online]. Available: https://revibeenergy.com/

[2] Broadsens Corporation. (2021, Dec) Wireless vibration and temperature sensors. Accessed on 2021-12-03. [Online]. Available: https://www.broadsens.com/sensors/wireless-low-power-sensors/

[3] Treon Oy. (2022, Jan) Treon industrial node 6. Accessed on 2022-01-05. [Online]. Available: https://www.treonstore.com/treon-industrial-node-6.html

[4] Perpetuum Ltd. (2021, Dec) Perpetuum. Accessed on 2021-12-03. [Online]. Available: https://perpetuum.com/

[5] Erbessd Instruments. (2022, Mar) Erbessd instruments. Accessed on 2022-03-20. [Online]. Available: https://www.erbessd-instruments.com/

[6] SKF. (2022, Mar) Condition monitoring systems. Accessed on 2022-03-20. [Online]. Available: https://www.skf.com/uk/products/condition-monitoring-systems

[7] P. Spies, M. Pollak, and L. Mateu, *Handbook of energy harvesting power supplies and applications.* CRC Press, 2015.

[8] P. Escobedo, I. P. de Vargas-Sansalvador, M. Carvajal, L. Capitán-Vallvey, A. Palma, and A. Martínez-Olmos, "Flexible passive tag based on light energy harvesting for gas threshold determination in sealed environments," *Sensors and Actuators B: Chemical*, vol. 236, pp. 226–232, 2016. [Online]. Available: https://doi.org/10.1016/j.snb.2016.05.158

[9] F. M. Discenzo, D. Chung, and K. A. Loparo, "Pump condition monitoring using self-powered wireless sensors," *Sound and Vibration*, vol. 40, pp. 12–15, 2006.

[10] G. Park, T. S. Rosing, M. D. Todd, C. R. Farrar, and W. S. Hodgkiss, "Energy harvesting for structural health monitoring sensor networks," *Journal of Infrastructure Systems*, vol. 14, pp. 64–79, 2008. [Online]. Available: https://doi.org/10.1061/(ASCE)1076-0342(2008)14:1(64)

[11] S. Ha and F. Chang, "Review of energy harvesting methodologies for potential shm applications," in *Proc., 2005 Int. Workshop on Structural Health Monitoring*, 2005, pp. 1451–1460.

[12] A. Davies, *Handbook of condition monitoring: techniques and methodology.* Springer Science & Business Media, 2012.

[13] A. F. Alessandra Di Pietro, Giuseppe Rotondo. (2018, dec) Capacitive MEMS accelerometer for condition monitoring. Accessed on 2022-10-10. [Online]. Available: https://www.st.com/content/ccc/resource/technical/document/white_paper/group0/c0/30/46/2f/00/24/42/1c/Capacitive_MEMS_accelerometer_for_condition_monitoring/files/MEMS_Condition_monitoring.pdf/jcr:content/translations/en.MEMS_Condition_monitoring.pdf

[14] STMicroelectronics. (2020, jun) ST sensor solutions for condition monitoring and predictive maintenance. Accessed on 2022-04-03. [Online]. Available: https://www.rutronik.com/fileadmin/Rutronik/Specials/Digital_SensorTest/Predictive_maintenance___3v3_Short__Rutronik.pdf

[15] ST Microelectronics. (2022, Mar) IIS3DWB datasheet: Ultra-wide bandwidth, low-noise, 3-axis digital vibration sensor. Accessed on 2022-03-22. [Online]. Available: https://www.st.com/content/ccc/resource/technical/document/datasheet/group3/14/0e/2b/1d/77/d0/46/f6/DM00501492/files/DM00501492.pdf/jcr:content/translations/en.DM00501492.pdf

[16] X. Tang, X. Wang, R. Cattley, F. Gu, and A. D. Ball, "Energy harvesting technologies for achieving self-powered wireless sensor networks in machine condition monitoring: A review," *Sensors*, vol. 18, no. 12, 2018. [Online]. Available: https://doi.org/10.3390/s18124113

[17] G. J. Snyder, *Thermoelectric Energy Harvesting*. Boston, MA: Springer US, 2009, pp. 325–336. [Online]. Available: https://doi.org/10.1007/978-0-387-76464-1_11

[18] S. Wojtczuk and K. Reinhardt, "High-power density (1040 W/kg) GaAs cells for ultralight aircraft," in *Conference Record of the Twenty Fifth IEEE Photovoltaic Specialists Conference-1996*, 06 1996, pp. 49 – 52.

[19] Planet Analog. Intel researchers demo RF energy harvester. Accessed on 2022-04-20. [Online]. Available: https://www.planetanalog.com/intel-researchers-demo-rf-energy-harvester/

[20] M. N. Fakhzan and A. G. A. Muthalif, "Vibration based energy harvesting using piezoelectric material," in *2011 4th International Conference on Mechatronics (ICOM)*, 2011, pp. 1–7.

[21] Xidas. (2022, mar) VEG vibration-based energy harvesting generator. Accessed on 2022-03-05. [Online]. Available: https://www.mouser.se/pdfDocs/Xidas_VEG_DS.pdf

[22] R. Aljadiri, L. Taha, and P. Ivey, "Electrostatic energy harvesting systems: A better understanding of their sustainability," *Journal of Clean Energy Technologies*, vol. 5, pp. 409–416, 09 2017.

[23] S. Anton and H. Sodano, "A review of power harvesting using piezoelectric materials (2003-2006)," *Smart Materials and Structures*, vol. 16, p. R1, 05 2007.

[24] J. M. Gilbert and F. Balouchi, "Comparison of energy harvesting systems for wireless sensor networks," *International Journal of Automation and Computing*, vol. 5, pp. 334–347, 2008.

[25] Revibe Energy AB. Electromagnetic vs. piezoelectric vibration energy harvesting. Accessed on 2022-03-20. [Online]. Available: https://revibeenergy.com/piezoelectric-electromagnetic-harvesting/?msclkid=2c0796c8a91911ecacfd4928032d0104

[26] David Squires, Squires Consulting. (2015, Feb) Energy harvesting for low-power sensor systems. Accessed on 2022-04-21. [Online]. Available: https://www.renesas.com/eu/ja/document/whp/energy-harvesting-low-power-sensor-systems

[27] M. Collotta, G. Pau, T. Talty, and O. K. Tonguz, “Bluetooth 5: A concrete step forward toward the IoT,” *IEEE Communications Magazine*, vol. 56, no. 7, pp. 125–131, 2018.

[28] A. Nikoukar, S. Raza, A. Poole, M. Güneş, and B. Dezfouli, “Low-power wireless for the internet of things: Standards and applications,” *IEEE Access*, vol. 6, pp. 67 893–67 926, 2018.

[29] Nordic Semiconductor. (2022, Apr) nRF52840 product specification. Accessed on 2022-04-21. [Online]. Available: https://infocenter.nordicsemi.com/index.jsp?topic=%2Fstruct_nrf52%2Fstruct%2Fnrf52840.html

[30] D. Gascón. (2022, Apr) 802.15.4 vs zigbee. Accessed on 2022-04-20. [Online]. Available: https://www.libelium.com/libeliumworld/802-15-4-vs-zigbee/

[31] Analog Devices. (2022) LTC3331 datasheet and product information. Accessed on 2022-03-22. [Online]. Available: https://www.analog.com/en/products/ltc3331.html

[32] Texas Instruments. (2022) Ultra low power harvester power management IC with boost charger, and nanopower buck converter. Accessed on 2022-03-22. [Online]. Available: https://www.ti.com/product/BQ25570

[33] ST Microelectronics. (2022) Ultra low power energy harvester and battery charger with embedded MPPT and LDOs. Accessed on 2022-03-22. [Online]. Available: https://www.st.com/en/power-management/spv1050.html

[34] Xidas. (2022) Xidas IoT. Accessed on 2022-04-14. [Online]. Available: https://www.xidasiot.com/power/ehm

[35] Nordic Semiconductor. (2022, mar) nrf52840 dongle. Accessed on 2022-03-22. [Online]. Available: https://www.nordicsemi.com/Products/Development-hardware/nrf52840-dongle

[36] IETF. (2022, Mar) IPv6 over bluetooth(r) low energy: Rfc 7668. Accessed on 2022-03-16. [Online]. Available: https://datatracker.ietf.org/doc/rfc7668/

[37] Xidas. (2022, mar) VP3 vibration perpetual power pod demo. Accessed on 2022-03-05. [Online]. Available: https://www.youtube.com/watch?v=E3j28-X_9Qc

[38] PCB Piezotronics. (2022, mar) Smartshaker™ with integrated power amplifier. Accessed on 2022-03-05. [Online]. Available: https://www.modalshop.com/excitation.asp?P=SmartShaker%E2%84%A2_with_Integrated_Power_Amplifier&ID=272

[39] D. H. Litwhiler, “A custom vibration test fixture using a subwoofer,” in *Proceedings of the 2011 IAJC-ASEE International Conference*, 2011, pp. 1–11. [Online]. Available: https://ijme.us/cd_11/PDF/Paper%2068%20ENT%20205.pdf

[40] PCB Piezotronics, Inc. (2022, apr) 333B30 | Accelerometer, ICP®. Accessed on 2022-04-21. [Online]. Available: https://www.pcb.com/products?model=333b30

[41] Analog Devices. (2022, mar) Adp5091/adp5092 datasheet. Accessed on 2022-03-05. [Online]. Available: https://www.analog.com/media/en/technical-documentation/data-sheets/ADP5091-5092.pdf

[42] Xidas. (2022, mar) Vp3 vibration perpetual power pod. Accessed on 2022-03-05. [Online]. Available: https://www.mouser.se/pdfDocs/Xidas_VP3_DS.pdf

[43] Nordic Semiconductor. (2022, may) Online power profiler for bluetooth le. Accessed on 2022-05-25. [Online]. Available: https://devzone.nordicsemi.com/power/w/opp/2/online-power-profiler-for-bluetooth-le

[44] Texas Instruments. (2022, apr) CC2640R2F Datasheet. Accessed on 2022-04-03. [Online]. Available: https://www.ti.com/lit/ds/symlink/cc2640r2f.pdf?ts=1655297384018&ref_url=https%253A%252F%252Fwww.google.com%252F

A

Appendix: PSU PCB Design Files

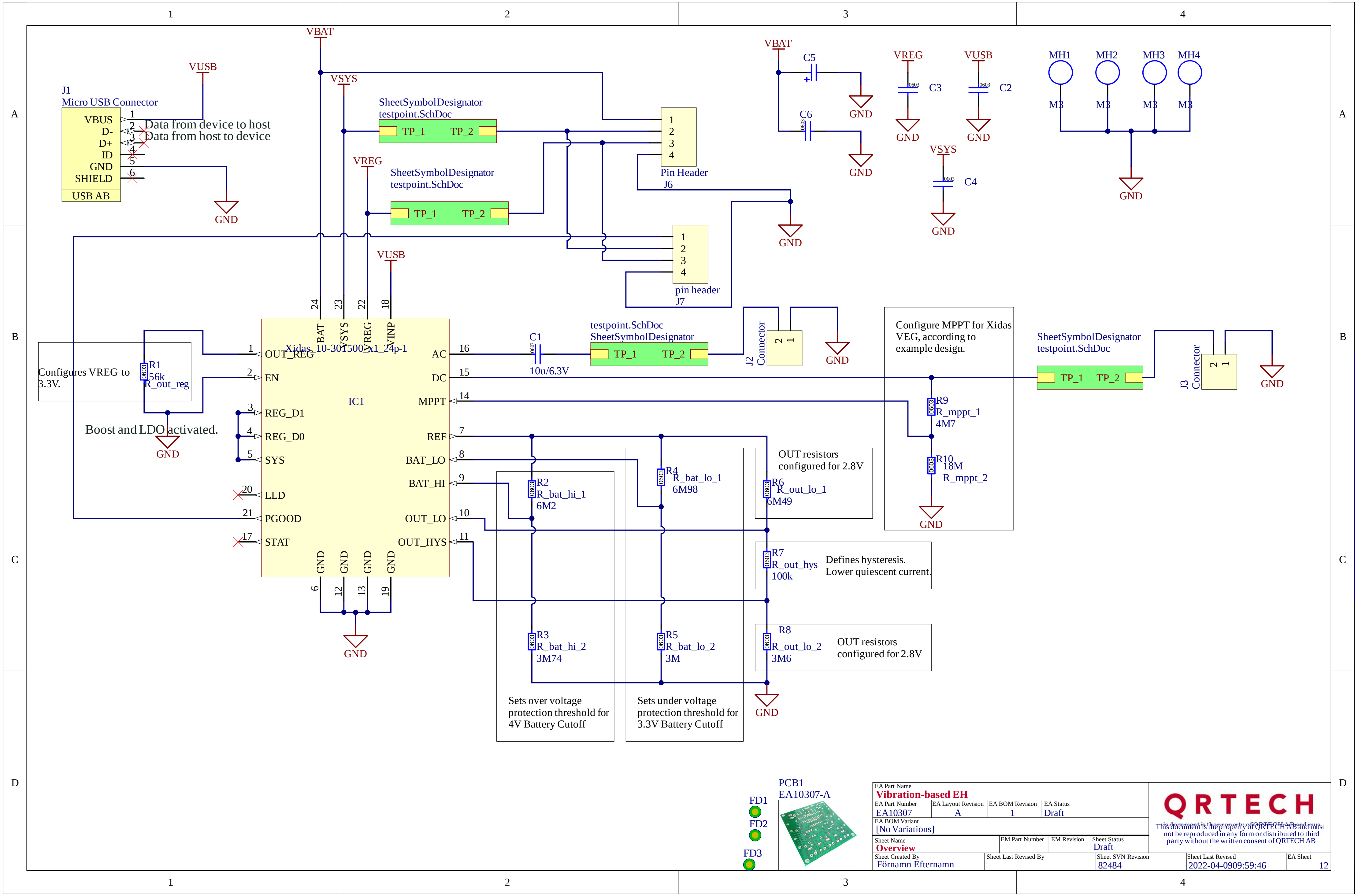

J1
Micro USB Connector
VBUS
D-
D+
ID
GND
SHIELD
USB AB
Data from device to host
Data from host to device
VUSB
VBAT
VSYS
VREG
GND
SheetSymbolDesignator
testpoint.SchDoc
TP_1
TP_2
Pin Header
J6
pin header
J7
Configures VREG to 3.3V.
R1
56k
R_out_reg
Boost and LDO activated.
Xidas_10-301500_x1_24p-1
IC1
OUT_REG
EN
REG_D1
REG_D0
SYS
LLD
PGOOD
STAT
BAT
VSYS
VREG
VINP
AC
DC
MPPT
REF
BAT_LO
BAT_HI
OUT_LO
OUT_HYS
C1
10u/6.3V
J2
Connector
J3
Connector
C5
C6
C3
C2
C4
MH1
MH2
MH3
MH4
M3
Configure MPPT for Xidas VEG, according to example design.
R9
R_mppt_1
4M7
R10
18M
R_mppt_2
R2
R_bat_hi_1
6M2
R3
R_bat_hi_2
3M74
Sets over voltage protection threshold for 4V Battery Cutoff
R4
R_bat_lo_1
6M98
R5
R_bat_lo_2
3M
Sets under voltage protection threshold for 3.3V Battery Cutoff
OUT resistors configured for 2.8V
R6
R_out_lo_1
6M49
R7
R_out_hys
100k
Defines hysteresis. Lower quiescent current.
R8
R_out_lo_2
3M6
OUT resistors configured for 2.8V
FD1
FD2
FD3
PCB1
EA10307-A
EA Part Name
Vibration-based EH
EA Part Number
EA10307
EA Layout Revision
A
EA BOM Revision
1
EA Status
Draft
EA BOM Variant
[No Variations]
Sheet Name
Overview
EM Part Number
EM Revision
Sheet Status
Draft
Sheet Created By
Förnamn Efternamn
Sheet Last Revised By
Sheet SVN Revision
82484
Sheet Last Revised
2022-04-0909:59:46
EA Sheet
12
QRTECH
This document is the property of QRTECH AB and must not be reproduced in any form or distributed to third party without the written consent of QRTECH AB

SheetSymbolDesignator

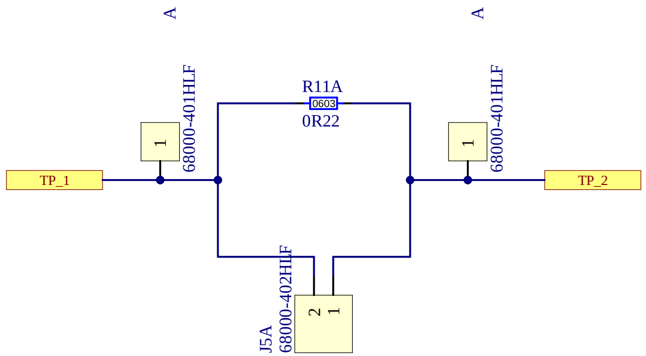

[Design Specification]()

Operating Temperature: -x°C to y°C

EA Part Name: Vibration-based EH				QRTECH
EA Part Number: EA10307	EA Layout Revision: A	EA BOM Revision: 1	EA Status: Draft	
EA BOM Variant: [No Variations]				This document is the property of QRTECH AB and must not be reproduced in any form or distributed to third party without the written consent of QRTECH AB
Sheet Name	EM Part Number	EM Revision	Sheet Status: Draft	
Sheet Created By: Förnamn Efternamn	Sheet Last Revised By	Sheet SVN Revision: 82413	Sheet Last Revised: 2022-04-0909:59:46	EA Sheet: 22

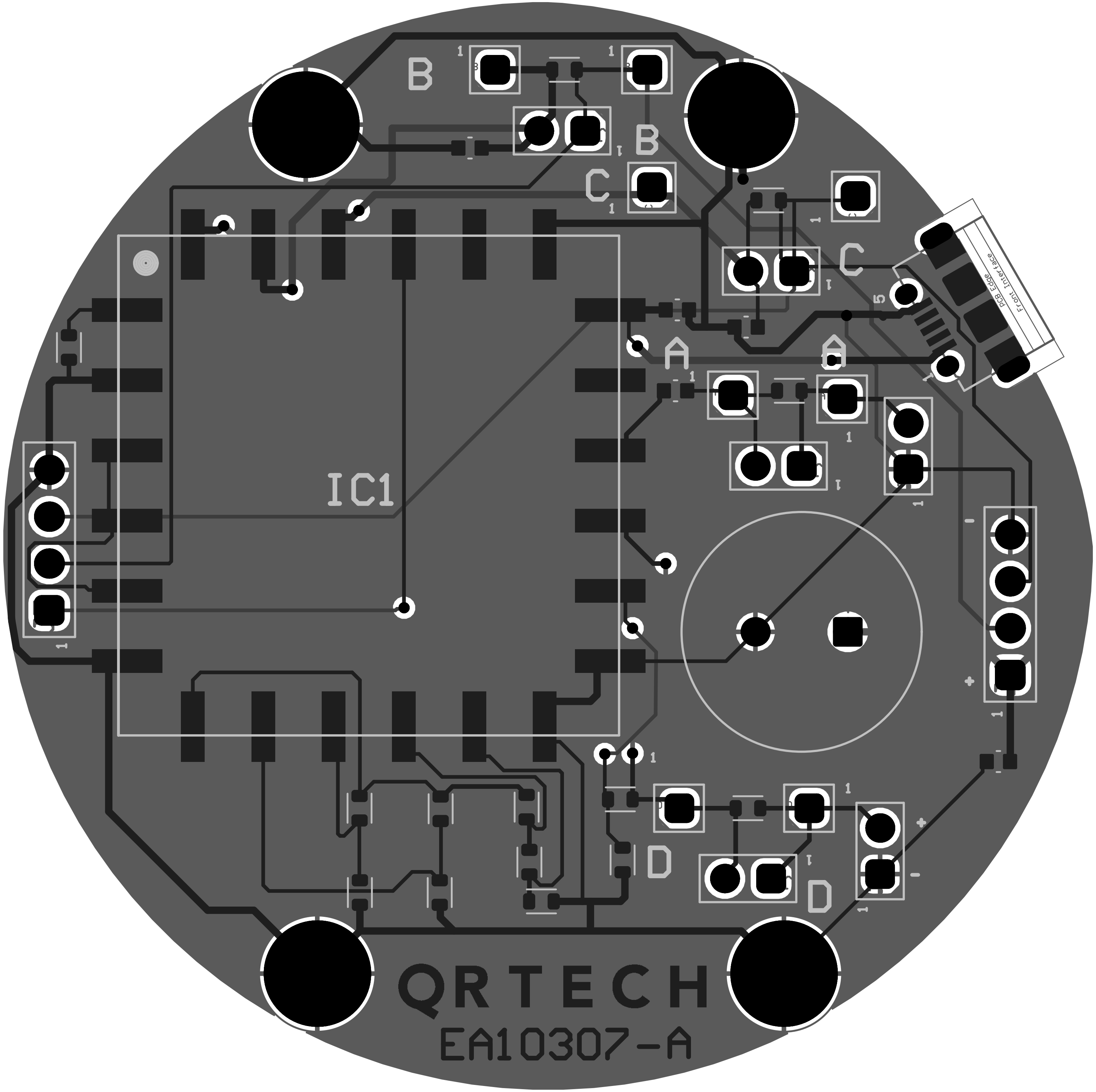
B
B
C
C
A
A
IC1
D
D
QRTECH
EA10307-A

B

Appendix: Test Rig PCB Design Files

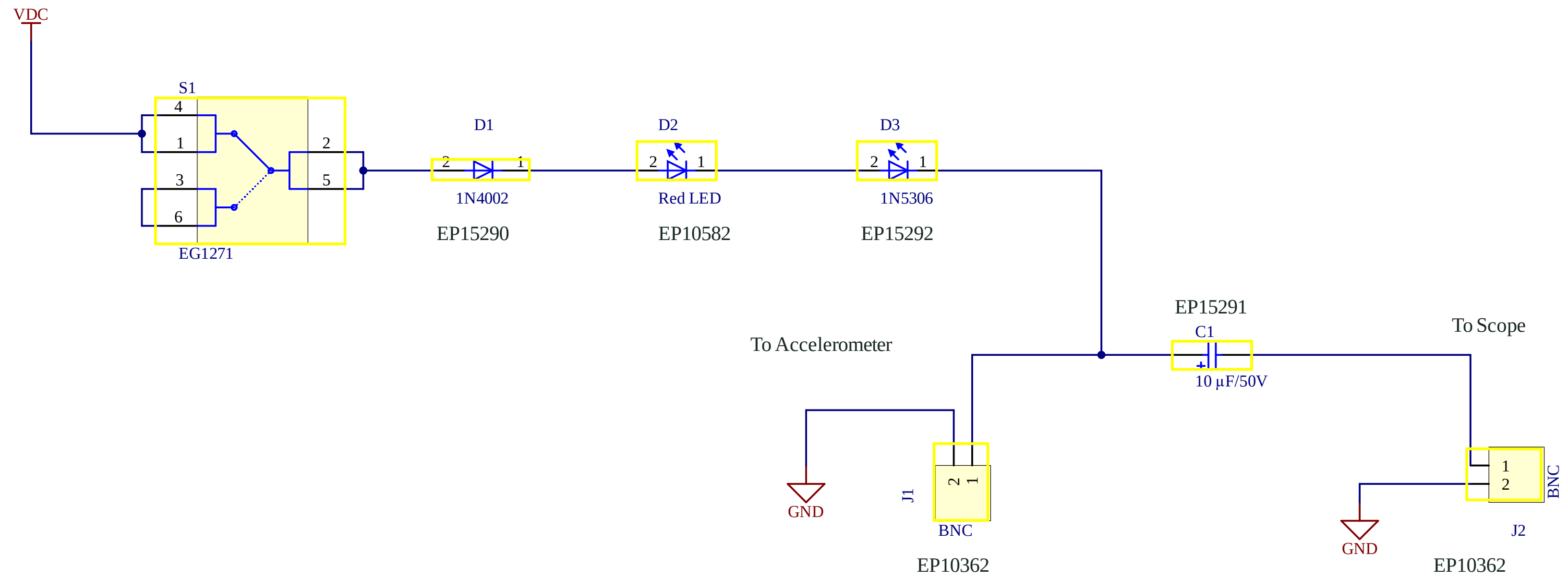

PCB1
EA10311-A

Design Specification

Operating Temperature: -x°C to y°C

EA Part Name			
VEH Test Board			
EA Part Number EA10311	EA Layout Revision A	EA BOM Revision 1	EA Status Draft
EA BOM Variant [No Variations]			
Sheet Name Overview	EM Part Number	EM Revision	Sheet Status Draft

Sheet Created By	Sheet Last Revised By	Sheet SVN Revision	Sheet Last Revised	EA Sheet
Rakshitha Madhusudhan	Erik Almbratt	82680	2022-04-2514:34:46	11

QRTECH

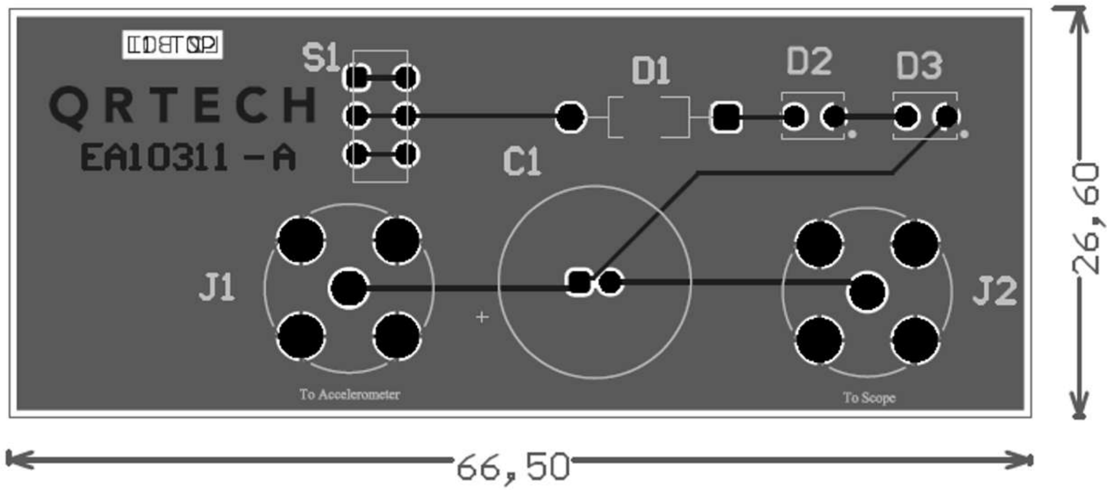

QRTECH
EA10311 - A
S1
D1
D2
D3
C1
J1
J2
To Accelerometer
To Scope
66,50
26,60

C

Appendix: Alternative nRF52840 Power Estimations

Table C.1: Average power consumption of nRF52840 during BLE transmission according to Nordic's Online Power Profiler for BLE [43]. Voltage: 3.3 V. Radio TX power: 8 dBm. PHY = 2 Mbps.

Phase	**Time** [µs]	**Current** [mA]	**Power** [mW]
Radio switch	150	3.3	10.89
Radio RX	44	6.5	21.45
Radio switch	140	3.5	11.55
Radio TX	148	15.1	49.83
Average		7.27	24.00

Table C.2: Average power consumption of nRF52840 during BLE transmission according to Nordic's Online Power Profiler for BLE [43]. Voltage: 3.3 V. Radio TX power: 4 dBm. PHY = 2 Mbps.

Phase	**Time** [µs]	**Current** [mA]	**Power** [mW]
Radio switch	150	3.3	10.89
Radio RX	44	6.5	21.45
Radio switch	140	3.5	11.55
Radio TX	148	10.2	33.66
Average		5.77	19.04

Exported settings from Nordic's Online Power Profiler for Bluetooth LE.

opp-params-ble.json:


```json
{
  "chip": "2",
  "voltage": "3.3",
  "dcdc": "on",
  "lf_clock": "lfxo",
  "radio_tx": "8",
  "ble_type": "con",
  "ble_int": "100",
  "tx_size": "216",
  "rx_size": "0",
  "phy": "1mbps",
  "slave_latency": "0",
  "central_ppm": "20",
  "peripheral_ppm": "20"
}
```